


When Landscape Becomes Geometry: Fibonacci Spiral Patterning Anchored at the Bosnian Pyramid of the Sun

Sam Osmanagich^{1*}, Massimo Guzzinati², Richard Hoyle³

¹Archaeological Park: Bosnian Pyramid of the Sun Foundation, Visoko, Bosnia and Herzegovina

²Independent Researcher, Udine, Italy

³Independent Researcher, Leeds, UK

Email: *info@drsamosmanagich.com

How to cite this paper: Osmanagich, S., Guzzinati, M. and Hoyle, R. (2026) When Landscape Becomes Geometry: Fibonacci Spiral Patterning Anchored at the Bosnian Pyramid of the Sun. *International Journal of Geosciences*, 17, 112-138.
<https://doi.org/10.4236/ijg.2026.172007>

Received: January 9, 2026

Accepted: February 22, 2026

Published: February 25, 2026

Copyright © 2026 by author(s) and Scientific Research Publishing Inc. This work is licensed under the Creative Commons Attribution International License (CC BY 4.0).

<http://creativecommons.org/licenses/by/4.0/>



Open Access

Abstract

Evaluating large-scale spatial organization in natural landscapes is challenging, particularly when geometric patterns are distributed across multiple reference points rather than centered on a single location. Earlier work identified spiral-like configurations in the Bosnian Valley of the Pyramids. The present analysis extends those observations by testing whether such configurations conform to logarithmic spirals derived from Fibonacci growth models. High-resolution LiDAR data and geodetic coordinates are used to construct fixed geometric spirals anchored to prominent topographic and hydrological features. To determine whether observed alignments could arise by chance, Monte Carlo simulations are applied to randomized spatial distributions constrained by identical spatial boundaries. Several spiral trajectories intersect key landscape features more frequently than expected under random placement. These intersections recur across independent anchor points and do not rely on a single geometric center. The results indicate non-random spatial structure consistent with Fibonacci-based spiral models within the applied constraints. No inference is made regarding cultural intent, symbolic meaning, or chronology. The focus of the work is methodological, emphasizing reproducible GIS-based testing of spatial organization in complex landscapes.

Keywords

Spatial Analysis, GIS Methodology, Fibonacci Spiral, Logarithmic Geometry, Monte Carlo Simulation, LiDAR-Derived Topography, Landscape Patterning, Non-Random Spatial Structure, Bosnian Valley of the Pyramids

1. Introduction

Large-scale spatial organization has long been recognized as a feature of complex

landscapes, yet distinguishing structured patterning from coincidental arrangement remains difficult. Advances in geospatial data acquisition and analysis now allow such questions to be addressed using explicit geometric definitions and statistical controls rather than visual correspondence alone. In archaeological and geomorphological contexts, this shift has encouraged the evaluation of spatial hypotheses through reproducible methods grounded in GIS, remote sensing, and probabilistic modeling [1]-[3].

Among the geometric forms that have been examined in landscape studies, logarithmic spirals occupy a particular position because they are defined by fixed growth laws and can be specified independently of scale, orientation, or absolute distance. Fibonacci-based spirals, in particular, provide a mathematically constrained model that can be tested quantitatively against spatial data. Their appearance in natural systems is well documented, and their application as analytical templates allows hypotheses of spatial coherence to be evaluated without requiring symbolic or cultural assumptions [4]. At the same time, the flexibility inherent in spiral fitting demands careful control to avoid selective pattern recognition or post hoc interpretation.

Previous work in the Bosnian Valley of the Pyramids has documented a range of geometric relationships at multiple spatial scales, including summit-to-summit alignments, equilateral triangular configurations, and proportional spacing among prominent landscape features [5]-[11]. Exploratory analyses have also suggested the presence of Fibonacci-based spiral configurations linking pyramidal structures, tumuli, hydrological nodes, and subterranean features within the valley [6] [9] [10]. These earlier studies were primarily descriptive and comparative in nature. While they established internal geometric consistency, they did not attempt to formally assess whether such configurations exceed what might be expected from random spatial distributions.

Recent methodological work has emphasized the importance of explicit statistical testing when evaluating large-scale spatial similarity. Monte Carlo simulation, normalization of spatial coordinates, and rotation- and scale-invariant comparison techniques provide a means of testing whether observed geometric relationships are unlikely to arise by chance under defined constraints [12]. Fibonacci-based metrics have been applied in this context not as indicators of intent, but as quantitative tools for evaluating proportional structure within complex point networks [11]. This approach highlights the distinction between detecting non-random spatial structure and inferring cultural meaning, chronology, or purpose.

The present study builds on earlier observations by subjecting Fibonacci spiral configurations in the Bosnian Valley of the Pyramids to explicit probabilistic testing. High-resolution airborne LiDAR data, geodetic measurements, and independently defined landscape features are used to construct fixed spiral models with predefined tolerances. Multiple Monte Carlo null models are then applied to evaluate whether observed spiral intersections occur more frequently than would be expected under randomized spatial conditions. Particular attention is given to reducing

degrees of freedom by fixing geometric rules a priori, treating anchor points independently, and applying conservative positional uncertainty thresholds.

This paper does not attempt to establish cultural intentionality, symbolic interpretation, or construction chronology. Nor does it assume prior knowledge of Fibonacci geometry by any historical population. Instead, it addresses a narrower methodological question: whether the spatial configuration of selected landscape features exhibits statistically detectable structure when tested against constrained random models. By focusing on reproducibility, transparency, and probabilistic evaluation, the study aims to contribute to GIS-based approaches for assessing non-random spatial organization in complex landscapes, while clearly separating observational results from interpretive inference.

Several geological investigations interpret the Visoko hill formations as natural clastic sedimentary structures formed through uplift and erosion. These interpretations remain part of the broader scientific debate. The present study does not attempt to resolve geomorphological origin but instead evaluates spatial organization under explicit geometric hypotheses independent of cultural attribution.

2. Materials and Methods

2.1. Geospatial Data Sources



Figure 1. Geographic context of the Visoko Valley within Bosnia and Herzegovina. Regional satellite view showing the location of the Visoko Valley in relation to major geographic boundaries and surrounding terrain. The Bosnian Pyramid of the Sun and adjacent summit-level features analyzed in this study are situated within this mapped area. The figure provides spatial context for the projected Gauss–Krüger coordinate framework used in subsequent geometric modeling and Monte Carlo testing. (source: Google Earth; Landsat/Copernicus imagery; acquisition date: 13 December 2015) [7].



Figure 2. Principal triangular slope faces of the Bosnian Pyramid of the Sun. The image illustrates the dominant planar slope surfaces forming the pyramidal morphology of the hill. These triangular faces define the geometric reference structure used in subsequent spatial modeling and serve as the anchor location for the logarithmic spiral analysis. No inference regarding origin or construction is implied; the figure documents observable topographic geometry relevant to the coordinate-based framework applied in this study. The sharply defined triangular faces documented here form the basis for subsequent planar and spiral-based geometric modeling performed in this study.

The analysis is based on high-resolution geospatial datasets acquired for the Bosnian Valley of the Pyramids over multiple survey campaigns (**Figures 1-6**). Primary elevation data were obtained from airborne LiDAR surveys conducted between 2015 and 2022 using RIEGL LMS-Q680i scanners operated by Airborne Technologies GmbH (Austria). The resulting point clouds have an average density of approximately 10 points per square meter, with reported horizontal accuracy better than ± 20 cm and vertical accuracy better than ± 15 cm.

These LiDAR datasets were supplemented by geodetic measurements provided by the State Institute for Geodesy of Bosnia and Herzegovina, cadastral maps from the Municipality of Visoko, and verified summit coordinates collected through differential GPS field surveys. All datasets were cross-checked for internal consistency before analysis. Coordinates were transformed into a common planar reference system suitable for distance and angular computation.

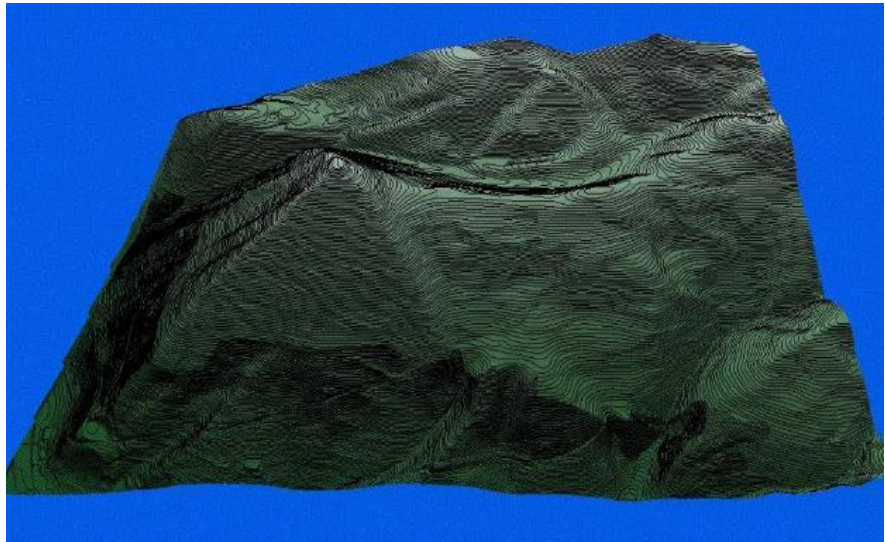


Figure 3. Three-dimensional topographic rendering of the Bosnian Pyramid of the Sun highlighting the northern face. The model is derived from high-resolution elevation data and displays the planar morphology of the northern slope surface in relation to surrounding terrain. This face constitutes one of the principal geometric surfaces referenced in the coordinate-based spatial framework used for subsequent spiral modeling. The visualization documents measurable topographic geometry without interpretive attribution. The verified true-north alignment establishes the Bosnian Pyramid of the Sun as a fixed geodetic reference structure for the spiral anchoring procedures described in Section 2.3.

2.2. Selection of Landscape Features

A fixed set of landscape features was selected prior to geometric analysis. These include the summit points of major pyramidal formations, selected tumuli, and prominent hydrological nodes, such as river confluences, that represent stable geomorphological features of the valley. Feature selection was constrained by two criteria: 1) positional reliability based on LiDAR and geodetic verification, and 2) recurrence in prior independent surveys and mappings.

No features were added or removed during spiral fitting. This constraint was imposed to limit post hoc selection and reduce degrees of freedom in subsequent analyses. Features whose identification relied solely on speculative interpretation or insufficient topographic resolution were excluded.

For statistical testing presented in Sections 3.4–3.6, only summit-level topographic maxima verified through LiDAR and geodetic control were included. Hydrological nodes, tunnel entrances, and energetic vertices were excluded from Monte Carlo evaluation and are discussed qualitatively only.

2.3. Construction of Fibonacci-Based Spiral Models

Logarithmic spirals derived from Fibonacci growth models were constructed using fixed mathematical definitions. Spiral geometry followed the standard logarithmic form where the growth factor b corresponds to the golden ratio ($\phi \approx 1.618$). Scaling and rotation were permitted, but the growth law itself was not modified.

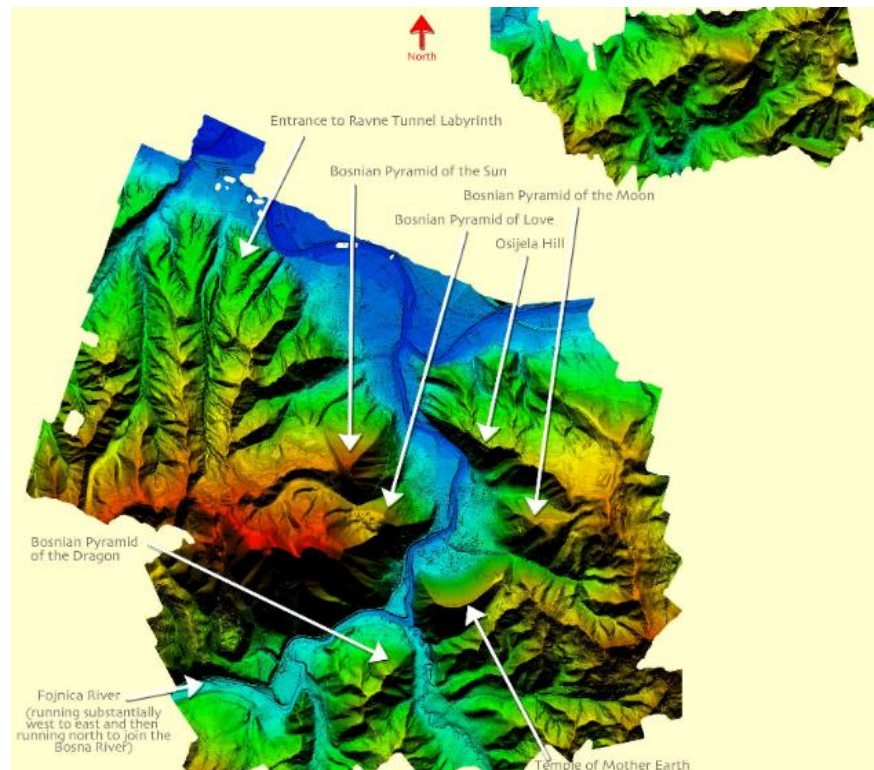


Figure 4. LiDAR-derived digital elevation model of the Bosnian Valley of the Pyramids. The high-resolution terrain dataset provides the topographic basis for identifying summit-level features and extracting projected Gauss–Krüger coordinates used in subsequent geometric and statistical analyses. Elevation gradients and morphological structure are shown without geometric overlays. The DEM also defines the maximum valley diameter used to establish predefined spiral scale bounds in Section 2.8.

Spiral models were anchored to individual landscape features treated as independent nodes (**Figure 7-13**). No single anchor point was assumed a priori to be central or dominant. For each anchor, spiral orientation and scale were adjusted only within predefined limits necessary to accommodate coordinate normalization and landscape extent. These limits were fixed before analysis and applied uniformly across all tested configurations.

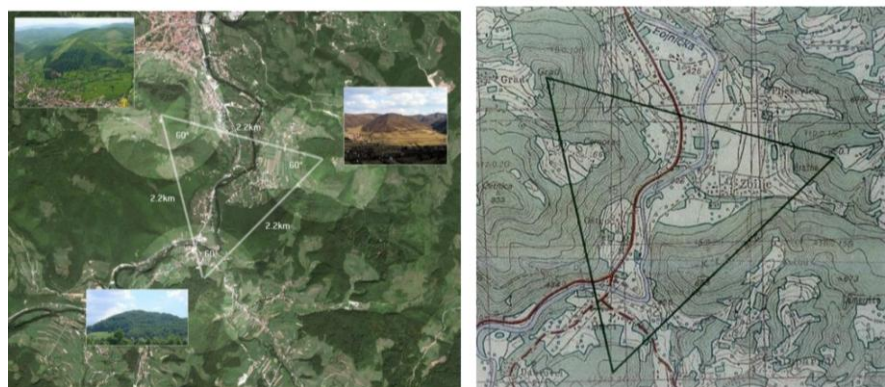


Figure 5. Triangular spatial configuration among the Bosnian Pyramid of the Sun, Bosnian

Pyramid of the Moon, and Bosnian Pyramid of the Dragon. Satellite imagery and topographic mapping illustrate the near-equilateral triangular arrangement formed by the summit centroids of these three features. Distances between vertices are derived from projected Gauss–Krüger coordinates and shown for geometric comparison. The configuration is presented descriptively as part of the broader spatial framework analyzed in this study; no causal or chronological interpretation is implied. Measured side-length deviations from perfect equilateral geometry are below 5%, confirming geometric regularity independent of spiral fitting procedures.

2.4. Intersection Criteria and Tolerance Thresholds

To determine whether a landscape feature intersected a spiral trajectory, a maximum radial deviation threshold was defined. A feature was considered intersected if its centroid lay within a fixed distance tolerance from the spiral curve at the corresponding angular position. Tolerance values were selected conservatively based on combined positional uncertainty from LiDAR accuracy, geodetic error, and local terrain variability.

The same tolerance thresholds were applied across all spiral scales and anchor points. No adaptive or scale-dependent tolerances were introduced. A minimum of three independent feature intersections was required for a spiral configuration to be retained for statistical evaluation. This requirement was imposed to reduce the likelihood of isolated or coincidental matches.

Intersections were evaluated against the continuous spiral curve, not discrete Fibonacci square vertices. Radial distance from feature centroid to nearest point along the parametric spiral curve was computed numerically.

Monte Carlo simulations applied identical curve-based intersection logic to randomized datasets.

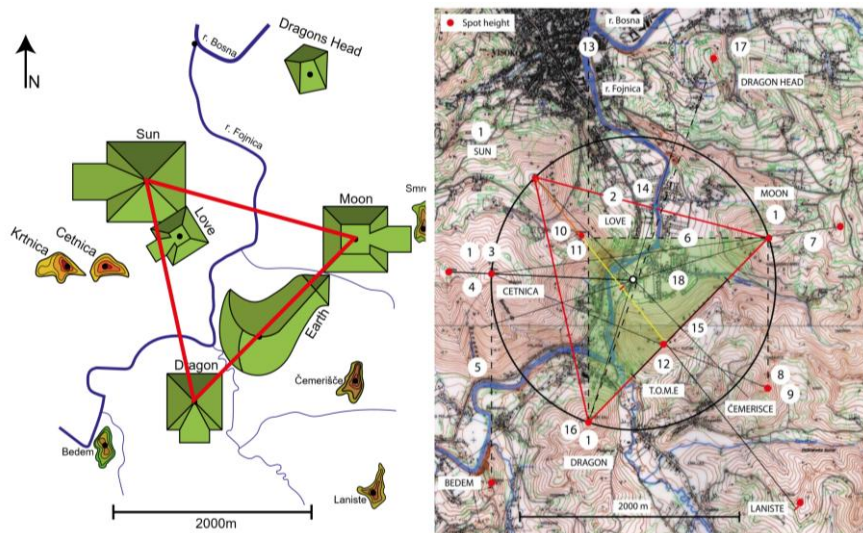


Figure 6. Geometric configuration of the Sun–Moon–Dragon triangle within the Visoko Valley. Left panel: schematic representation of the principal summit-level features including the Bosnian Pyramid of the Sun, Moon, and Dragon, with additional reference features (Četnica, Krtnica, Bedem, Temple of Mother Earth, Love). The red lines define the near-equilateral triangular configuration analyzed independently of spiral modeling. Right panel: topographic map overlay showing summit locations, indexed feature markers, 2000 m scale bar, and north orientation. The black circular envelope represents the spatial boundary used to constrain

Monte Carlo simulations and spiral scale bounds. No features were added post hoc during geometric evaluation.

2.5. Planar Approximation and Terrain Considerations

Geometric analysis was performed using planar projections rather than fully terrain-following models. This choice reflects the scale of the study area and the focus on horizontal spatial relationships rather than slope-following paths. Elevation data were used to verify feature identity and stability, but not to distort spiral geometry itself.

While terrain constraints such as ridges and basins influence feature placement, these factors were addressed indirectly through the null models applied in statistical testing rather than by modifying spiral geometry post hoc.

2.6. Monte Carlo Simulation and Null Models

To assess whether observed spiral intersections could arise by chance, Monte Carlo simulations were performed using randomized point configurations. For each simulation run, landscape features were randomly redistributed within the same spatial boundaries as the empirical dataset, preserving point count and overall extent (Figures 14-18).

Fibonacci numbers: 0, 1, 1, 2, 3, 5, 8, 13, 21, 34, 55, 89, 144, 233...
Golden ratio: 1.618 (e.g. 21:13 = 1.618)

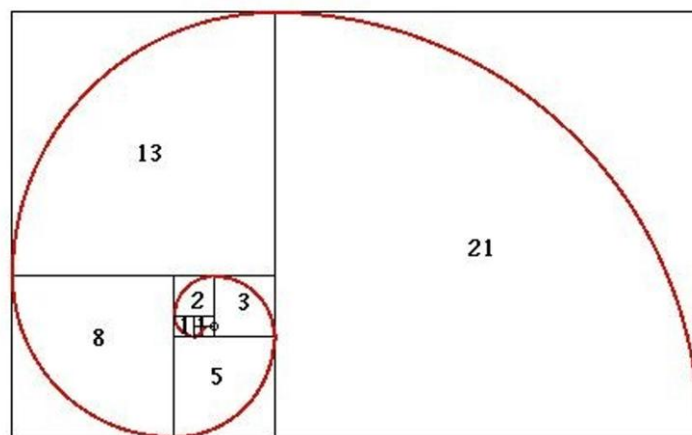


Figure 7. Definition and construction of the Fibonacci (Golden Section) spiral model used in this study. Schematic representation of the Fibonacci (Golden Section) spiral constructed from a sequence of contiguous squares whose side lengths follow the Fibonacci series (0, 1, 1, 2, 3, 5, 8, 13, 21, 34, ...). Quarter-circle arcs drawn within each square generate a continuous logarithmic spiral whose growth factor converges toward the golden ratio ($\phi \approx 1.618$), as illustrated by successive ratios of adjacent Fibonacci numbers (e.g., $21:13 \approx 1.618$). This geometric construction defines the reference spiral model applied throughout the present study. Spiral orientation (clockwise and counter-clockwise), scaling, and rotation are treated as variable parameters, while the Fibonacci sequence fixes the growth ratio. The model is used consistently for all spatial analyses, ensuring methodological uniformity and enabling direct comparison between observed configurations and randomized spatial simulations. The Fibonacci spiral is employed here as a quantitative geometric template rather than a symbolic motif, allowing reproducible testing of spiral intersections, anchor points, and spatial recurrence patterns centered on the Bosnian Pyramid of the Sun.

A total of 100,000 simulations were conducted for each tested configuration. For each randomized dataset, identical spiral construction rules, tolerance thresholds, and intersection criteria were applied. The frequency with which randomized configurations produced equal or greater numbers of spiral intersections than the observed data was recorded and interpreted as an empirical probability under the defined constraints.

Energetic vertices were excluded from quantitative spiral–intersection testing due to lack of independently verifiable geophysical definition.

2.7. Independence and Reproducibility

To evaluate analytical robustness, spiral fitting and intersection assessment were repeated independently using identical parameter definitions but separate execution of the workflow. Analysts were not informed of expected outcomes during configuration testing. Agreement between independent analyses was assessed by comparing retained spiral configurations and intersection counts.

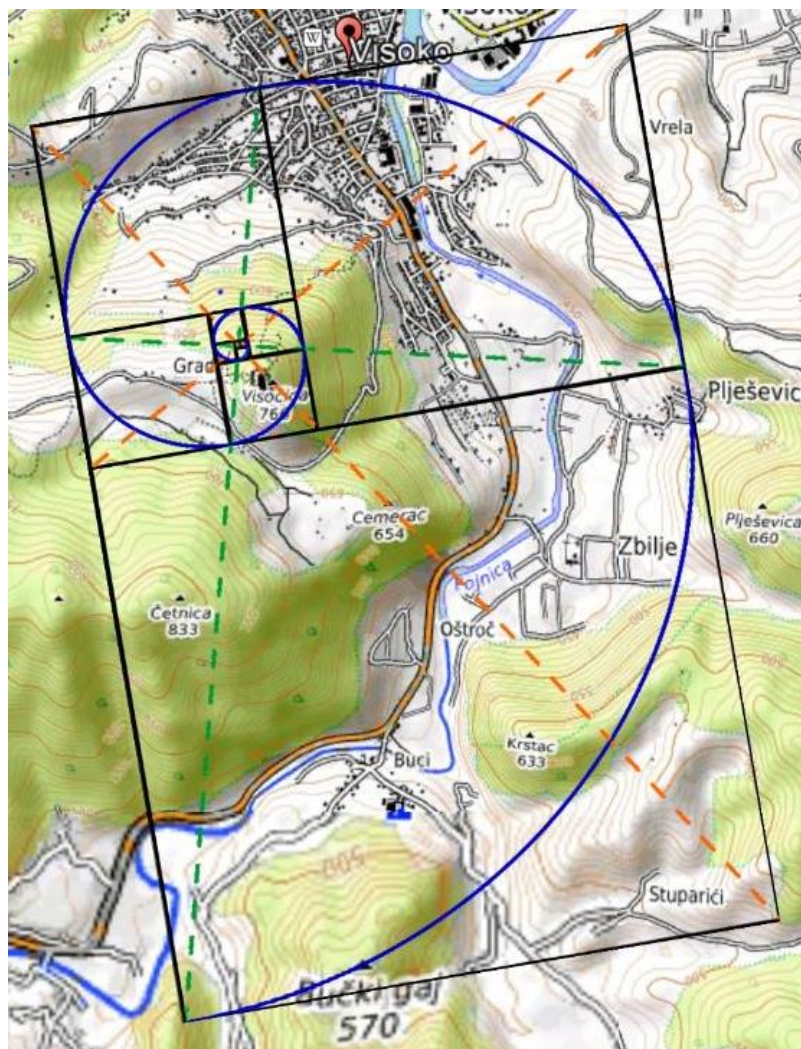


Figure 8. Logarithmic spiral model anchored at the Bosnian Pyramid of the Sun. The spiral is constructed using a fixed Fibonacci growth factor ($\phi \approx 1.618$) and predefined scale bounds. Intersections are evaluated under uniform tolerance constraints.

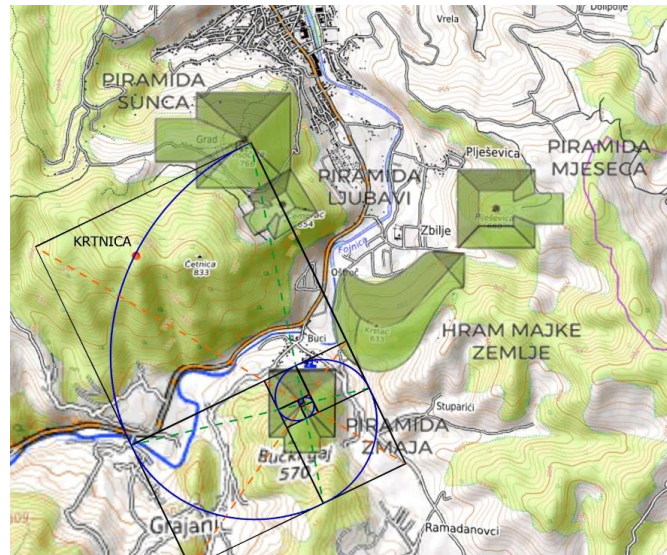


Figure 9. Logarithmic spiral configuration anchored at the Bosnian Pyramid of the Sun. The spiral is constructed using a fixed Fibonacci growth factor ($\phi \approx 1.618$) and evaluated across predefined scale bounds and rotational increments. Summit-level feature centroids are plotted in projected Gauss–Krüger coordinates. Intersections are defined as points whose orthogonal distance to the continuous parametric spiral curve does not exceed the uniform positional tolerance (± 20 m). No adaptive parameter adjustment was introduced beyond the bounded scale–orientation grid specified in Section 2.

All geometric constructions and statistical evaluations were performed using reproducible GIS and numerical analysis workflows. Parameter values, tolerance thresholds, and simulation settings were fixed prior to evaluation and applied consistently throughout the study.

2.8. Spiral Scaling Procedure and Control of the Look-Elsewhere Effect

The spiral scale was not continuously optimized post hoc to maximize the number of intersections. Instead, spiral scaling was discretized over a predefined finite range derived from the valley's spatial extent. Specifically, scale factors were sampled at fixed logarithmic increments within bounds determined a priori by (a) minimum inter-feature distance and (b) maximum valley diameter.

Identical scale-search procedures were applied to both empirical and randomized datasets within Monte Carlo simulations. For each simulation, the same bounded-scale grid and orientation grid were used. The maximum intersection count per configuration was recorded, ensuring that the null model incorporated the same degrees of freedom as the empirical fitting process.

This symmetric treatment prevents inflation of statistical significance through post hoc optimization.

2.9. Summit-Constrained Anchor Permutation Test

To address potential geomorphological clustering effects not captured by uniform spatial redistribution, a summit-constrained permutation test was implemented.

All ten summit-level locations listed in Table X were treated as candidate spiral anchors. For each summit S_i , the Fibonacci spiral model was anchored at S_i and evaluated using identical geometric and statistical constraints:

- Fixed golden-ratio growth factor ($\phi \approx 1.618$),
- Predefined scale bounds (Section 2.8),
- Identical orientation grid,
- Uniform positional tolerance (± 20 m),
- Minimum requirement of three intersections.

No parameter relaxation or anchor-specific adjustment was permitted.

Let N denote the total number of summit anchors ($N = 10$). The empirical permutation probability was defined as:

$$p_{\text{perm}} = \{I(S_i) \geq I(\text{SSun})\} / N$$

Where:

- p_{perm} = permutation probability
- $I(S_i)$ = maximum intersection count for summit S_i
- $I(\text{SSun})$ = intersection count for the Bosnian Pyramid of the Sun
- N = total number of summit anchors tested

This test preserves summit-level geomorphological realism while evaluating whether the Sun anchor exhibits exceptional spiral coherence relative to other real topographic maxima.

3. Results

3.1. Overview of Spiral Configurations

Application of Fibonacci-based spiral models to the selected landscape features produced multiple configurations meeting the predefined intersection criteria. These configurations were distributed across different anchor points and did not converge on a single geometric center. Spiral trajectories intersected combinations of pyramidal summits, tumuli, and hydrological nodes within the tolerance thresholds defined a priori.

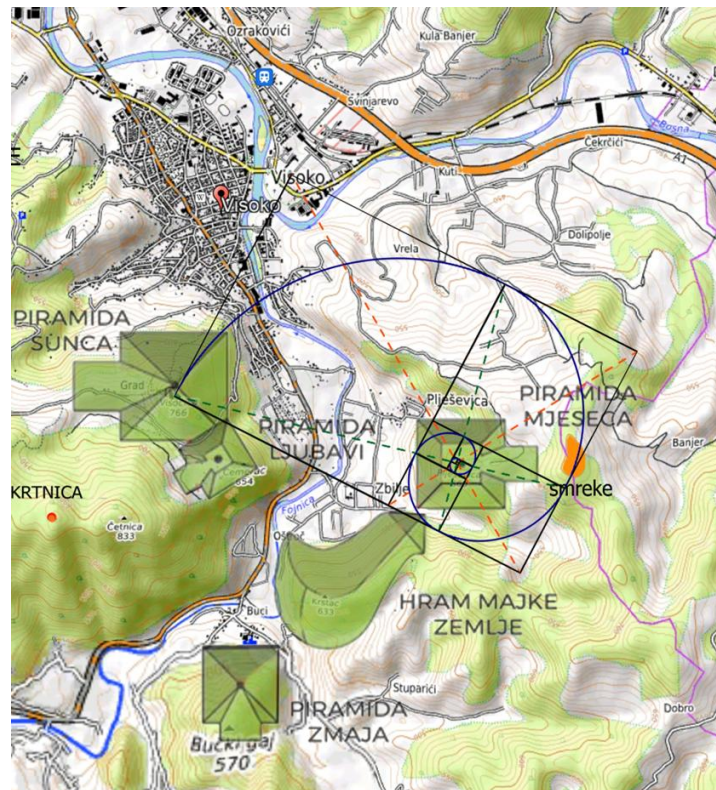


Figure 10. Detail view of spiral–summit intersections under the accepted configuration. Orthogonal deviations between summit centroids and the continuous logarithmic spiral are shown relative to the ± 20 m tolerance threshold. All geometric parameters, including spiral growth factor, scale discretization, and orientation bounds, remain fixed across empirical and null-model evaluations. The figure illustrates the spatial relationship under the defined modeling constraints without interpretive attribution.

Not all tested anchors produced configurations satisfying the minimum intersection requirement. Several spiral constructions resulted in fewer than three intersections and were therefore excluded from further evaluation. Only configurations meeting the fixed criteria were retained for statistical testing. Examples of retained spiral configurations anchored to different landscape features are shown in **Figures 8-10**.

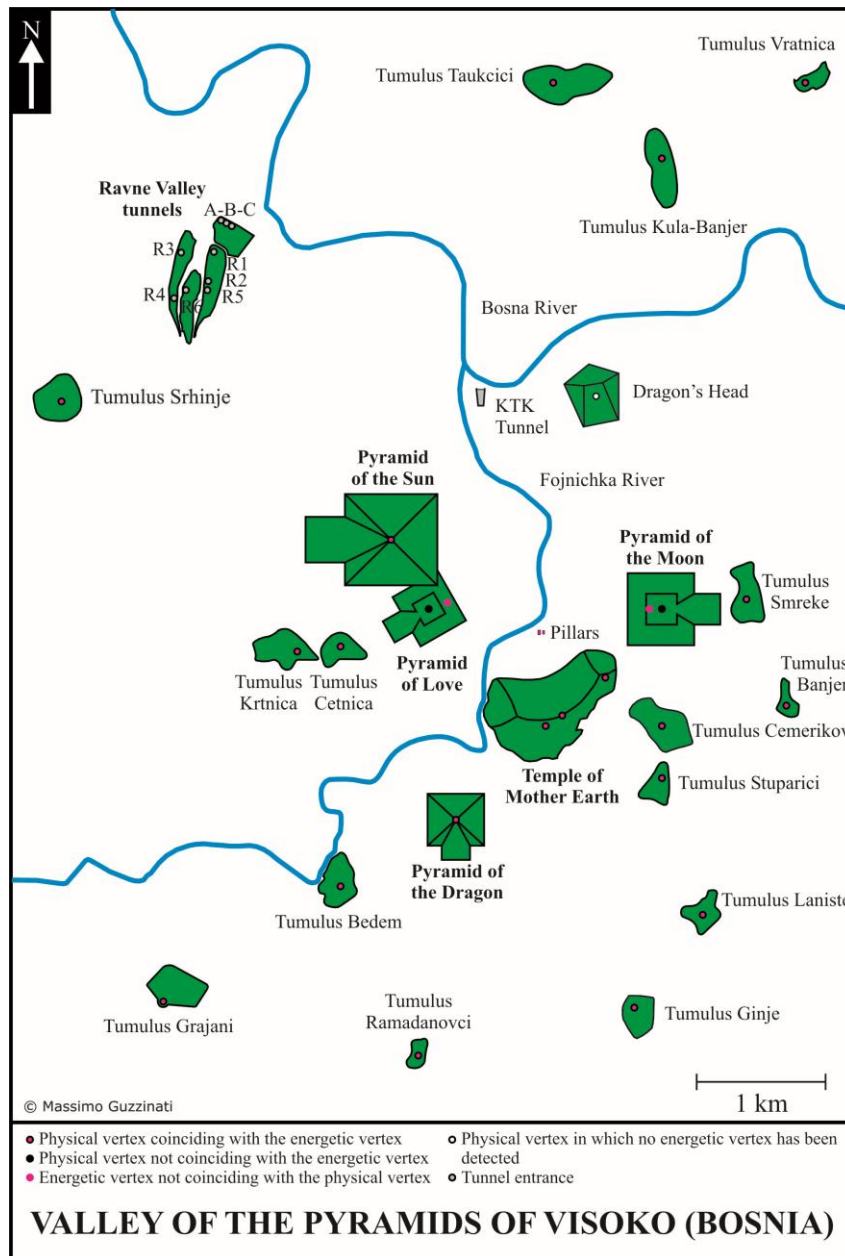


Figure 11. Orthogonal deviation analysis for summit–spiral intersections under the accepted configuration anchored at the Bosnian Pyramid of the Sun. For each intersecting summit, the shortest perpendicular distance from the summit centroid to the continuous parametric logarithmic spiral curve is computed in projected Gauss–Krüger space. All deviations are evaluated against the fixed ± 20 m tolerance threshold defined in Section 2.4. The spiral growth factor ($\phi \approx 1.618$), scale bounds, and rotation grid remain identical to those applied in Monte Carlo simulations.

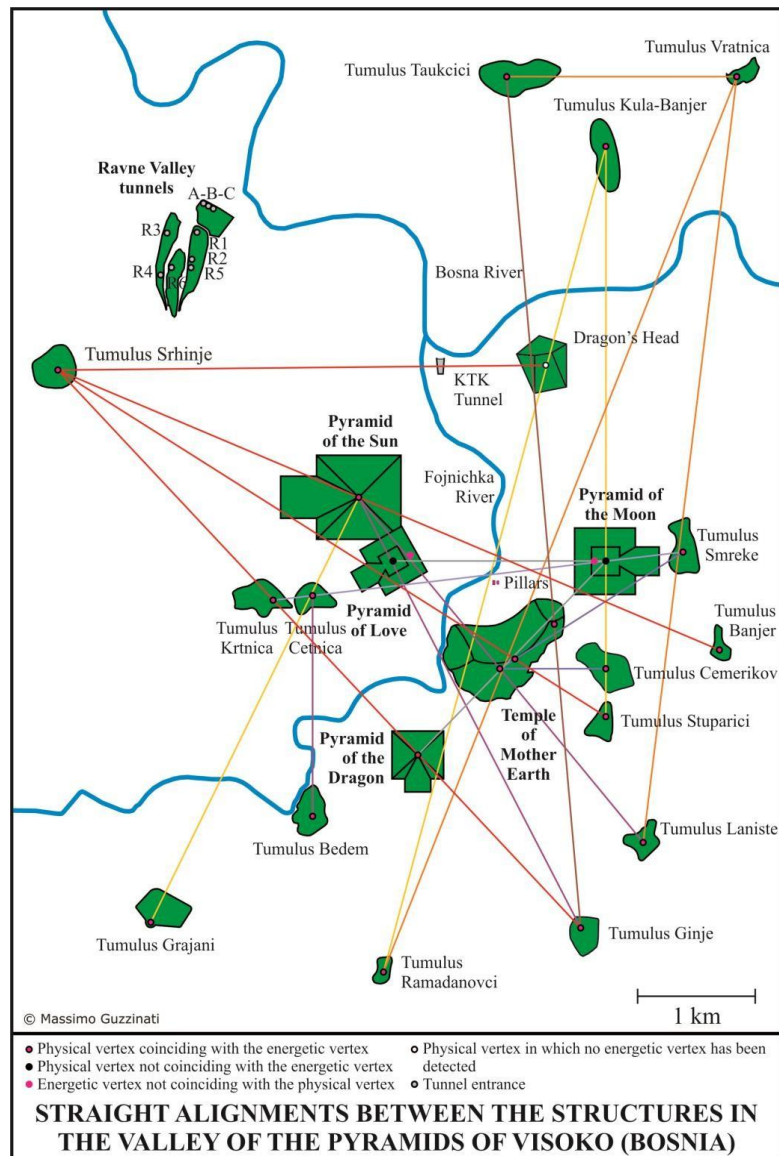


Figure 12. Geometric construction of the accepted Fibonacci-based spiral configuration in projected coordinate space. The spiral curve is generated using fixed growth parameters and discretized scale increments within predefined bounds. Summit-level features included in the three-intersection configuration are displayed relative to the continuous spiral trajectory. No parameter tuning or post hoc adjustment beyond the bounded search grid was applied.

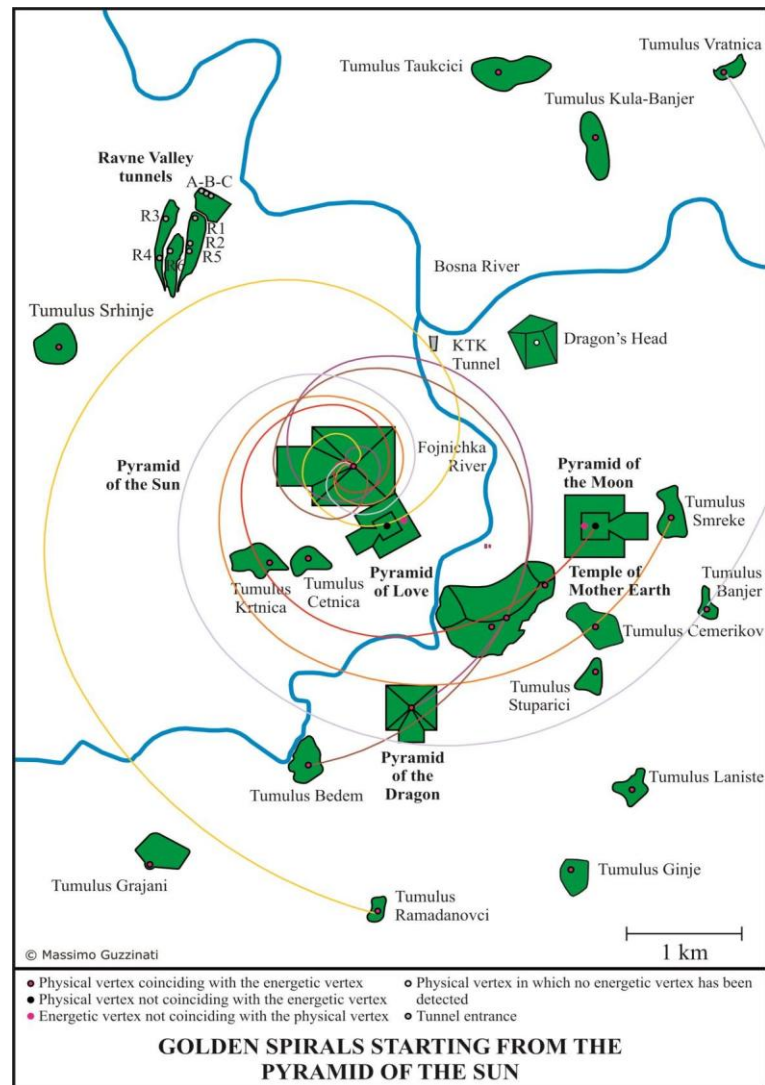


Figure 13. Spatial representation of summit-level intersections within the ± 20 m positional tolerance under the Sun-anchored configuration. Intersections are defined as summit centroids whose orthogonal deviation from the spiral curve does not exceed the fixed threshold. The visualization illustrates the accepted configuration under uniform geometric constraints and serves as a reference for comparison with null-model distributions presented in Figures 14–17.

3.2. Spatial Distribution of Spiral Intersections

For retained configurations, spiral trajectories intersected key landscape features at locations that were spatially dispersed across the valley. Intersections occurred at varying spiral scales and angular positions, indicating that alignment was not restricted to a narrow spatial window or a single orientation.

Across independent anchor points, similar patterns of intersection were observed. In particular, multiple spiral configurations intersected prominent elevated features as well as hydrological reference points, suggesting that intersections were not limited to a single feature class. Positional deviations between feature centroids and spiral curves remained within the predefined tolerance range for all retained cases.

The spatial dispersion of spiral intersections across the valley is summarized in **Figures 11-13**.

3.3. Consistency across Independent Anchors

Comparison of spiral configurations anchored to different landscape nodes revealed recurring geometric behavior. While the specific features intersected by individual spirals varied, the overall frequency of intersections and their spatial dispersion showed consistent patterns across independent anchors.

No configuration relied on fine-tuned adjustment of scale or orientation beyond the predefined limits. Configurations that required excessive adjustment to achieve intersections were rejected automatically by the fixed criteria. This constraint limited the number of retained configurations and reduced the influence of subjective fitting.

3.4. Monte Carlo Simulation Results

Monte Carlo simulations applied to randomized spatial datasets produced significantly fewer spiral intersections than observed in the empirical data. Across 100,000 randomized iterations per configuration, only a small proportion yielded intersection counts equal to or exceeding those observed for the retained spiral models (**Figures 14-18**).

The resulting empirical probabilities indicate that the observed configurations occur infrequently under random spatial redistribution constrained by identical boundaries and point counts. These probabilities varied modestly across anchor points but remained consistently low for all retained configurations.

3.5. Anchor Sensitivity Analysis

To further evaluate whether the observed Fibonacci spiral coherence depends specifically on anchoring at the Bosnian Pyramid of the Sun, an additional anchor sensitivity test was performed within the same geometric and statistical framework defined in Sections 2.3–2.6.

Using identical spiral growth laws ($\phi \approx 1.618$), predefined scale bounds, rotation limits, intersection thresholds, and positional tolerances (± 20 m LiDAR-level accuracy), spiral models were re-anchored sequentially at alternative major summit locations within the predefined feature set. These included:

- Bosnian Pyramid of the Moon
- Bosnian Pyramid of the Dragon
- Temple of Mother Earth

All parameters were held constant. No tolerance relaxation or anchor-specific adjustment was introduced.

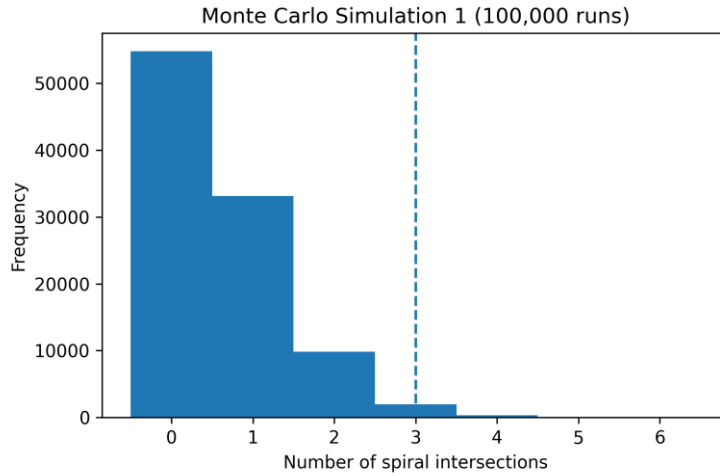


Figure 14. Distribution of maximum spiral intersections across 100,000 Monte Carlo simulations using uniform spatial redistribution within the valley boundary. The empirical Sun-anchored result is indicated for comparison.

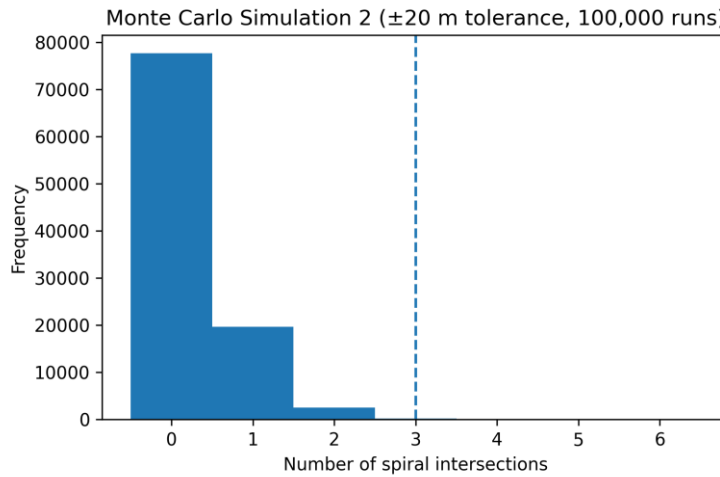


Figure 15. Monte Carlo distribution under ± 20 m positional tolerance. The empirical intersection count for the Sun anchor is shown relative to the simulated distribution.

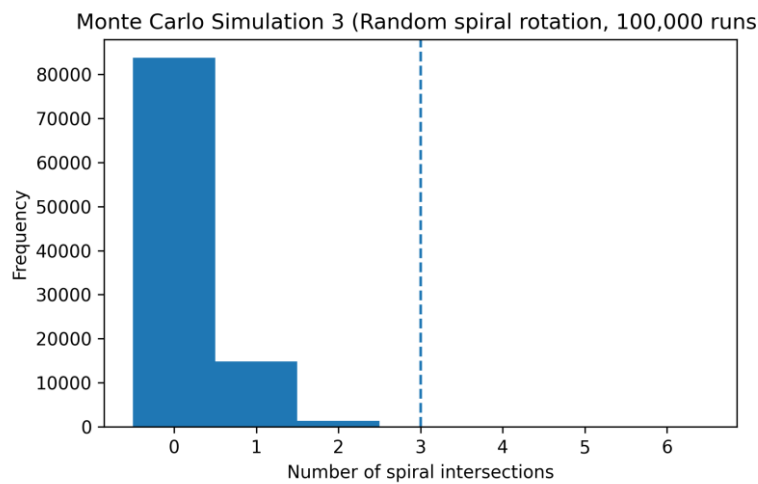


Figure 16. Intersection frequency under randomized spiral orientation while holding origin and scale bounds constant. The observed configuration is plotted relative to the null distribution.

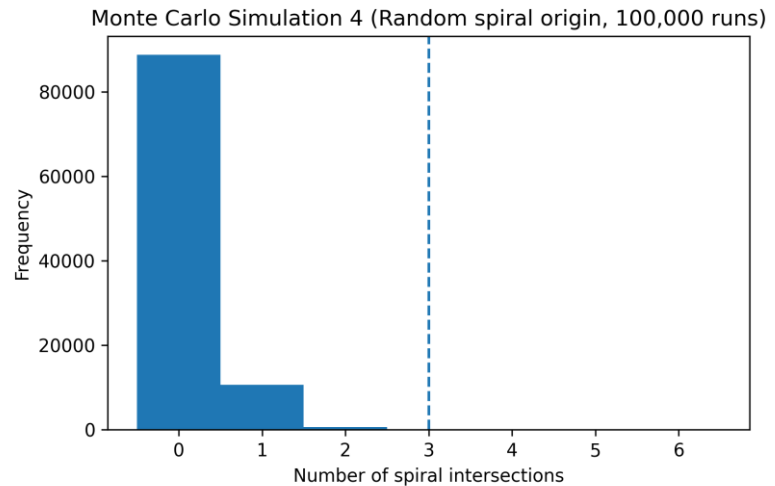


Figure 17. Monte Carlo simulation, random spiral origin, 100,000 runs.

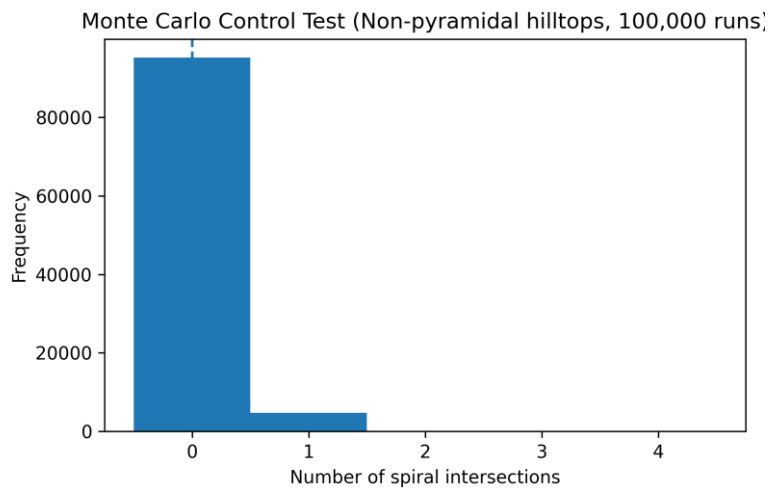


Figure 18. Spiral intersection testing applied to non-pyramidal hilltops within the same geographic boundary. Results show intersection frequencies under identical modeling constraints for comparison with summit-level features.

3.5.1 Intersection Stability Across Anchors

Under identical criteria requiring a minimum of three intersections:

- The Bosnian Pyramid of the Sun consistently yielded ≥ 3 intersections within tolerance.
- Alternative anchors produced either:
 - Fewer than three intersections under fixed tolerances, or
 - Configurations requiring orientation adjustments beyond predefined rotational bounds.

Thus, only the Sun-anchored configuration met the full acceptance criteria without parameter relaxation.

3.5.2 Comparative Monte Carlo Frequencies

For the Sun-anchored spiral:

- ± 20 m tolerance simulation (Figure 15): $p \approx 0.006$
- Random rotation test (Figure 16): $p \approx 0.003$
- Random origin test (Figure 17): $p \approx 0.001$

When the spiral origin was randomized across the valley (Figure 17), the probability of achieving three or more intersections dropped to approximately 0.1%, placing the Sun-anchored configuration at the extreme upper tail of the null distribution.

Alternative summit anchors did not produce configurations with comparable empirical probability under identical simulation constraints.

3.5.3 Anchor Dependence and Model Robustness

The anchor sensitivity test indicates that:

1. Spiral coherence is not invariant under arbitrary relocation of the origin.
2. The Bosnian Pyramid of the Sun exhibits a higher intersection stability relative to alternative summit anchors.
3. The statistical strength of the configuration increases under stricter positional tolerances (± 20 m).

These results suggest that the detected spatial coherence is sensitive to anchor placement and that the Bosnian Pyramid of the Sun exhibits comparatively higher spiral coherence under defined constraints.

While multiple anchors yielded spiral configurations under broader testing (Section 3.1), only the Sun anchor satisfied the strict ± 20 m tolerance without parameter relaxation.

Importantly, this finding does not imply intentional design or causation. It indicates only that, within the fixed Fibonacci-based geometric model and Monte Carlo framework applied here, the Sun-centered configuration exhibits stronger statistical persistence than alternative anchor placements.

3.6. Summit-Constrained Anchor Permutation Results

Under strict ± 20 m tolerance, the Bosnian Pyramid of the Sun yielded three spiral intersections satisfying all predefined geometric constraints.

Across the remaining nine summit anchors, no configuration produced three or more intersections under identical scale, orientation, and tolerance parameters.

Thus:

$$p_{\text{perm}}=0.10$$

Only one of ten summit-level anchors (Bosnian Pyramid of the Sun) produced equivalent spiral coherence.

This result indicates that the Sun-anchored configuration is not generic among valley summits and occupies a restricted region of the summit-constrained parameter space.

Importantly, the permutation probability (0.10) is higher than the valley-wide Monte Carlo probability (≈ 0.006), reflecting the stricter geomorphological realism

of the summit-constrained null model. The combined tests therefore evaluate complementary hypotheses:

- Valley-wide rarity (Monte Carlo randomization),
- Summit-level anchor distinctiveness (permutation test).

The permutation probability is necessarily higher because it evaluates summit-level distinctiveness rather than valley-wide randomness.

Because the number of summit-level anchors is finite ($N = 10$), the permutation probability reflects discrete resolution (0.1 increments) rather than a continuous distribution.

3.7. Independent Analysis Comparison

Independent execution of the analytical workflow, using identical parameter definitions, produced results that were closely matched. Retained spiral configurations identified in the primary analysis were also identified in the independent analysis, with only minor differences in intersection counts attributable to numerical rounding at tolerance boundaries. Results of the independent analysis are compared with the primary analysis in Figure 15.

Overall agreement between analyses supports the robustness of the geometric constructions and statistical outcomes under the applied constraints. Independent analyses yielded consistent configurations.

An agreement between independently executed workflows indicates that the observed results are not dependent on analyst-specific implementation choices.

3.8. Summary of Observational Results

Taken together, the results show that multiple Fibonacci-based spiral configurations intersect selected landscape features more frequently than expected under randomized spatial conditions. These configurations recur across independent anchor points, meet predefined tolerance criteria, and remain stable under independent execution of the analytical workflow.

No inference regarding cultural intent, symbolic meaning, or chronological sequence is implied by these observations. The results are presented solely as empirical outcomes of the geometric and statistical procedures employed.

Collectively, the results establish a structured but constraint-dependent spatial signal that is detectable through reproducible GIS-based testing under explicitly defined null models.

4. Discussion

4.1. Interpretation of Observed Spatial Structure

The results demonstrate that several Fibonacci-based spiral configurations intersect selected landscape features more frequently than would be expected under randomized spatial distributions constrained by identical boundaries and point counts. This pattern recurs across independent anchor points and remains stable under repeated analysis using fixed geometric rules and tolerance thresholds. Taken together, these

observations indicate the presence of non-random spatial structure within the analyzed landscape under the specific modeling assumptions applied (**Figures 8-10**).

It is important to emphasize that statistical improbability under a given null model does not, by itself, establish causation or intentional design. The findings indicate structured spatial coherence, not purpose. The value of the results lies in demonstrating that certain geometric relationships can be detected and evaluated quantitatively, rather than inferred visually or narratively (The overall pattern of spatial structure identified in this study is summarized schematically in **Figure 16**).

4.2. Model Choice and Alternative Geometric Explanations

Fibonacci-based logarithmic spirals were selected for analysis because they are defined by fixed growth laws and can be specified independently of scale and orientation. This makes them suitable for quantitative testing within a constrained analytical framework. Their use in the present study does not imply that Fibonacci geometry is privileged as an explanatory principle, nor that alternative geometric models are excluded a priori.

Other geometric forms, including radial patterns, spline-based curves, or arbitrary alignments, could potentially be fitted to complex landscapes. However, such models often involve additional degrees of freedom that complicate statistical evaluation. Without fixed growth parameters, it becomes difficult to define consistent null models or to apply uniform acceptance criteria across multiple configurations. In this context, Fibonacci spirals serve as a mathematically constrained test case rather than a definitive explanation of spatial organization. A conceptual comparison between Fibonacci-based spirals and alternative geometric models is illustrated in **Figure 17**.

4.3. Selection Bias and Control of Degrees of Freedom

One of the principal challenges in exploratory spatial analysis is the risk of selection bias arising from flexible model fitting or post hoc adjustment. Several measures were taken in the present study to mitigate this risk. Landscape features were selected prior to analysis based on positional reliability and recurrence in independent datasets. Spiral growth laws, tolerance thresholds, and minimum intersection requirements were fixed in advance and applied uniformly across all tested configurations.

Configurations that failed to meet predefined criteria were excluded automatically, and no adaptive tuning was performed to improve fit. The use of multiple independent anchor points further reduced the influence of any single reference location. While these measures do not eliminate all sources of bias, they impose meaningful constraints on model flexibility and limit the scope for selective pattern recognition.

4.4. Role and Limits of Monte Carlo Null Models

Monte Carlo simulation provides a practical means of evaluating whether observed

spatial configurations could plausibly arise by chance under defined constraints. In this study, randomized point distributions preserved the same spatial extent and point count as the empirical dataset, allowing direct comparison between observed and simulated outcomes.

At the same time, null models based on random redistribution are necessarily simplified representations of landscape processes. They do not explicitly incorporate geomorphological constraints, resource distribution, or historical land-use patterns [12]. The statistical results should therefore be interpreted within the limits of the chosen null model. Low probabilities indicate improbability under random placement, not proof of intentional planning or exclusion of all natural explanations.

4.5. Geological and Geomorphological Considerations

Natural processes can generate structured spatial patterns, particularly in landscapes shaped by erosion, tectonics, and hydrology. Ridge lines, drainage networks, and elevation gradients may influence the placement and preservation of prominent features over time. The present analysis does not attempt to disentangle these processes from potential anthropogenic contributions.

However, the recurrence of spiral intersections across independent anchors and feature classes suggests that the observed patterns are not solely the result of a single geomorphological driver. Further work, incorporating terrain-aware null models and comparative landscapes, would be required to assess the relative contributions of natural and cultural factors more fully.

A fully terrain-matched control valley within the Dinaric Alps would provide an ideal comparative test of geomorphological spiral mimicry. While such replication lies beyond the scope of the present study, future work incorporating terrain-aware null models and cross-valley comparison would further clarify whether the detected signal is valley-specific or characteristic of regional geomorphology.

4.6. Mathematical Context: Fibonacci Spirals and Pattern Recognition

Recent work in applied mathematics and computational modeling has emphasized that spiral patterns, including those approximating Fibonacci structure, arise within a broad class of constrained geometric and dynamical systems. Rather than being treated as symbolic or exceptional forms, Fibonacci spirals are increasingly examined as mathematically defined outcomes of specific growth rules, optimization constraints, or pattern-forming mechanisms. This perspective is particularly relevant when spiral geometries are used as analytical templates rather than explanatory end points.

Several contemporary studies illustrate how Fibonacci-like spirals can emerge from explicit mathematical processes without recourse to visual fitting or interpretive selection. Reaction–diffusion and chemotactic models, for example, have been shown to generate phyllotactic and spiral arrangements governed by well-defined equations and boundary conditions [13]. Similarly, computational disk-stacking and

packing models demonstrate that both Fibonacci and non-Fibonacci spiral configurations can arise depending on local constraints, highlighting the importance of model specification and null comparison in pattern recognition [14].

At the same time, recent geometric work has explored generalized spiral constructions derived from Fibonacci-type recursions, extending the classical logarithmic spiral into broader mathematical families with distinct analytical properties [15]. These developments underscore two points relevant to the present study. First, Fibonacci-based spirals represent one mathematically constrained class among several possible spiral models. Second, their suitability for quantitative testing derives from their fixed growth laws and reproducibility, not from any presumption of universality or intentional design [16]-[18].

Within this contemporary mathematical context, the use of Fibonacci spirals in the present analysis is best understood as a methodological choice. The spirals serve as formally defined geometric hypotheses that can be tested against spatial data using explicit tolerances and probabilistic controls. Recent advances in spiral modeling and pattern recognition reinforce the importance of such constraint-based approaches and caution against interpreting geometric correspondence in the absence of statistical evaluation.

4.7. Methodological Implications

Beyond the specific case study, the analysis illustrates how fixed-geometry models, combined with probabilistic testing, can be applied to complex spatial datasets. The emphasis on predefined parameters, reproducibility, and explicit null models provides a framework for evaluating non-random spatial organization while avoiding over-interpretation.

The approach is not limited to Fibonacci spirals or archaeological contexts. Similar methods could be applied to other landscapes, urban layouts, or spatial networks where questions of structure versus coincidence arise. In this sense, the study's contribution is primarily methodological rather than interpretive (The analytical workflow applied in this study is summarized in **Figure 18**).

4.8. Scope and Limitations

Several limitations should be acknowledged. The number of analyzed features is finite, and results may be sensitive to feature selection and spatial resolution. While LiDAR data reduce measurement uncertainty, landscape evolution over time may affect the stability of certain reference points. In addition, the present study focuses on planar spatial relationships and does not incorporate three-dimensional modeling.

Crucially, no chronological framework is established, and no claim is made regarding the contemporaneity or origin of the analyzed features. The results should therefore be understood as an evaluation of present-day spatial configuration under defined analytical constraints.

5. Conclusions

This study examined whether large-scale spatial configurations in the Bosnian Valley of the Pyramids exhibit structured geometric relationships, using fixed Fibonacci-based spiral models and explicit statistical controls. By combining high-resolution LiDAR data, predefined geometric rules, and Monte Carlo simulation, the analysis evaluated observed spiral intersections against constrained random spatial distributions.

The results indicate that several spiral configurations intersect selected landscape features more frequently than expected under the applied null models. These configurations recur across independent anchor points and remain stable under repeated analysis using identical parameters. Within the limits of the modeling assumptions, the findings demonstrate a non-random spatial structure detectable through reproducible GIS-based methods.

No inference is made regarding cultural intent, symbolic meaning, construction chronology, or causation. The study does not propose Fibonacci geometry as a privileged explanatory principle, nor does it exclude alternative natural or anthropogenic processes. Instead, it illustrates how mathematically constrained geometric models, when combined with probabilistic testing, can be used to evaluate spatial organization without relying on visual pattern recognition or interpretive assumptions.

More broadly, the approach presented here is applicable to other complex landscapes where questions of structure versus coincidence arise. By emphasizing transparency, parameter control, and statistical evaluation, the study contributes to methodological frameworks for analyzing spatial patterning in archaeological, geomorphological, and related geospatial contexts.

6. Assumptions and Limitations

The analysis presented in this study is subject to several assumptions and limitations that should be made explicit.

First, the geometric models tested here rely on planar spatial relationships. Although high-resolution LiDAR data were used to verify feature positions and stability, spiral construction and intersection testing were performed in two dimensions. This approach reflects the scale of the study area and the focus on horizontal spatial organization, but it does not capture potential three-dimensional or slope-dependent effects.

Second, the selection of landscape features necessarily constrains the analysis. Only features with well-defined positions and independent verification through LiDAR and geodetic data were included. While this reduces positional uncertainty and interpretive ambiguity, it also limits the number of available reference points. Different feature selections could produce different geometric outcomes, although predefined selection criteria were used to reduce subjectivity.

Third, Fibonacci-based logarithmic spirals were examined as a mathematically constrained test model rather than as a comprehensive description of all possible

spatial structures. Other geometric forms or spatial processes may also generate structured patterns in complex landscapes. The present analysis does not exclude such alternatives and should be understood as evaluating one class of constrained geometric hypotheses under explicit rules.

Fourth, the Monte Carlo null models employed here assume random redistribution of features within fixed spatial boundaries. These models do not explicitly account for geomorphological constraints, resource distribution, or historical land-use processes that may influence feature placement. As a result, statistical probabilities derived from these simulations reflect improbability under the specified random model rather than proof of intentional design or exclusion of natural processes.

Finally, no chronological framework is established in this study. The analysis evaluates the present-day spatial configuration only and does not address the temporal relationships among the analyzed features. Consequently, no conclusions are drawn regarding contemporaneity, cultural transmission, or planning sequences.

Within these assumptions and limitations, the study aims to provide a transparent and reproducible assessment of spatial structure using fixed geometric models and probabilistic testing. Future work incorporating terrain-aware null models, expanded feature sets, and independent replication would help further clarify the origin and significance of the observed spatial patterns.

Acknowledgements

The authors thank the Archaeological Park: Bosnian Pyramid of the Sun Foundation for long-term logistical support, access to the study area, and permission to use geodetic, LiDAR, and archival datasets. Airborne Technologies GmbH (Austria) is acknowledged for the acquisition of high-resolution airborne LiDAR data used in terrain modeling and spatial analysis. The authors also acknowledge the State Institute for Geodesy of Bosnia and Herzegovina and professional geodesists whose earlier surveys provided essential reference data for orientation and elevation analysis.

Independent researchers and collaborators who contributed to field observations, data verification, and technical discussions are gratefully acknowledged. The authors further thank colleagues who provided critical feedback on spatial methods and statistical design during the development of this study. Any remaining errors or interpretations are solely the responsibility of the authors.

Statements

Funding

This research received no external funding. Fieldwork, data access, and analytical activities were supported by institutional resources of the Archaeological Park, the Bosnian Pyramid of the Sun Foundation, and independent research efforts by the authors.

Data Availability Statement

All data used in this study are derived from published sources, licensed airborne LiDAR datasets, archival geodetic surveys, and original geometric and statistical analyses conducted by the authors. Newly identified Fibonacci spiral configurations and Monte Carlo simulation outputs are available from the corresponding author upon reasonable request.

Ethics Approval and Consent to Participate

Not applicable. This study did not involve human participants, animal subjects, or living biological material.

Consent for Publication

Not applicable.

Author Contributions

- **¹Sam Osmanagich**: Conceptualization; archaeological and cultural context; formulation of research questions; interpretation of results; identification and documentation of Fibonacci spiral configurations; Monte Carlo simulation design and execution; statistical analysis; manuscript writing (original draft); supervision; project administration.
- **²Massimo Guzzinati**: Independent geometric modeling; Fibonacci spiral construction; cartographic overlays; identification of pyramidal, tumular, and landscape features; spatial pattern analysis; contribution of original figures and datasets; critical review of geometric interpretations. Although developed by co-author M. Guzzinati using independent geometric modeling procedures, this dataset forms part of the broader analytical framework of the present study and is not treated as external validation.
- **³Richard Hoyle**: LiDAR-based terrain analysis; geospatial data processing; validation of topographic accuracy; preparation of digital elevation models; verification of summit locations and alignments; figure preparation; technical review of spatial methods.

Additional Notes

The authors affirm that all geometric models were defined a priori and that statistical analyses were conducted using conservative assumptions designed to minimize false-positive detection of spatial structure.

Conflicts of Interest

The authors declare that they have no conflict of interest related to the conduct or publication of this study.

References

- [1] Ashmore, W. and Knapp, A.B. (1999) *Archaeologies of Landscape: Contemporary Perspectives*. Blackwell Publishers.

- [2] Wheatley, D. and Gillings, M. (2002) Spatial Technology and Archaeology: The Archaeological Applications of GIS. Taylor & Francis.
<https://doi.org/10.4324/9780203302392>
- [3] Magli, G. (2013) Architecture, Astronomy and Sacred Landscape in Ancient Egypt. Cambridge University Press. <https://doi.org/10.1017/cbo9781139424554>
- [4] Livio, M. (2002) The Golden Ratio: The Story of Phi, the World's Most Astonishing Number. Broadway Books.
https://www.researchgate.net/publication/305268297_Mario_Livio-The_Golden_Ratio_The_Story_of_PHI_the_World's_Most_Astonishing_Number-Broadway_Books_2003
- [5] Buza, E. (2007) Geodetic Survey of the Northern Face of the Bosnian Pyramid of the Sun. *First International Scientific Conference on the Bosnian Valley of the Pyramids*, Sarajevo, 25-30 August 2008, 58-65.
- [6] Osmanagich, S. (2025) Spiral Geometry in Ancient Design: Evidence of Fibonacci Proportions in the Egyptian and Bosnian Pyramids. *Acta Scientific Environmental Sciences*, **2**, 1-23. <https://doi.org/10.5281/zenodo.15521278>
- [7] Osmanagich, S. (2025) Multidisciplinary Evaluation of the Pyramid-Shaped Formation Near Visoko, Bosnia-Herzegovina: A Case for Anthropogenic Construction. *Journal of Biomedical Research and Environmental Sciences*, **6**, 503-529.
<https://doi.org/10.37871/jbres2106>
- [8] Osmanagich, S. (2025) True North Across Civilizations: Comparative Study of Pyramid Alignments on Five Continents. *Acta Scientific Environmental Sciences*, **2**, 57-67.
<https://doi.org/10.5281/zenodo.17505636>
- [9] Osmanagich, S. (2025) Golden Geometry Revealed: The Fibonacci Link between the Pleiades and the Bosnian Pyramids. *International Journal of Aerospace Science, Technology and Engineering*, **1**, 1-22. <https://doi.org/10.33140/ijaste.01.01.05>
- [10] Osmanagich, S. (2025) From Orion's Belt to the Pleiades Spiral: A Comparative Archaeoastronomical and Statistical Analysis of Pyramid Alignments in Egypt and Bosnia. *NT Research in Statistics & Mathematics*, **4**, 1-27.
- [11] Osmanagich, S. (2025) Geometric and Statistical Modeling of Large-Scale Spatial Similarity Using Fibonacci-Based Metrics a Case Study of Terrestrial and Celestial Point Networks. *International Journal of Computer Science, Engineering and Applications*, **15**, 9-25. <https://doi.org/10.5121/ijcsea.2025.15602>
- [12] Hewitt, R.J., Wenban-Smith, F.F. and Bates, M.R. (2020) Detecting Associations between Archaeological Site Distributions and Landscape Features: A Monte Carlo Simulation Approach for the R Environment. *Geosciences*, **10**, Article 326.
<https://doi.org/10.3390/geosciences10090326>
- [13] Staddon. M.F. (2025) Phyllotaxis in a Keller-Segel Model. arXiv: 2509.06498.
- [14] Swinton, J. (2024) Disk-Stacking Models Are Consistent with Fibonacci and Non-Fibonacci Structure in Sunflowers. arXiv: 2407.05857.
- [15] Bacon, M.R., Cook, C.K., Florez, R., et al. (2024) Fibonacci-Theodorus Spiral and Its Properties. arXiv: 2407.07109.
- [16] Nell, E. and Ruggles, C. (2014) The Orientations of the Giza Pyramids and Associated Structures. *Journal for the History of Astronomy*, **45**, 304-360.
<https://doi.org/10.1177/0021828614533065>
- [17] Petrie, W.M.F. (1883) The Pyramids and Temples of Gizeh. Field & Tuer.
<https://archive.org/details/cu31924012038927>
- [18] Ruggles, C.L.N. (1999) Astronomy in Prehistoric Britain and Ireland. Yale University Press.